Preprint Title Phosphorous-doped green-emission fluorescent carbon dots sensing for pH, lemon yellow and the antioxidant application

Authors Xiaoliang Hao, Shujuan Dai, Zhigang Fang, Jing Guo and Yingxue Teng

Article Type Full Research Paper

ORCID® iDs Yingxue Teng - https://orcid.org/0000-0001-9158-4686

Phosphorous-doped green-emission fluorescent carbon dots sensing for pH, lemon yellow and the antioxidant application

Xiaoliang Hao[1], Shujuan Dai[2], Zhigang Fang[1], Jing Guo[3], Yingxue Teng[3,*]

[1]School of chemical engineering, University of Science and Technology Liaoning, Anshan 114051, PR China

[2]School of Mining Engineering, University of Science and Technology Liaoning, Anshan 114051, PR China

[3]School of Materials and Metallurgy, University of Science and Technology Liaoning, Anshan 114051, PR China

* Corresponding author. Email: liaoningkeda@ustl.edu.cn

* Corresponding author: Yingxue Teng

Abstract

In this paper, we reported green-emission carbon dots (CDs) using a single step hydrothermal carbonization. The CDs were prepared by m-phenylenediamine, tris, phosphoric acid, and pure water by heating for 8 h at 180 ℃. The CDs exhibited green-emission fluorescence, were sensitive to pH, and was successfully used analysed the pH of real water samples. Besides, the CDs could detect of food additive lemon yellow, with

the limit of detection as low as 0.13 μM. More importantly, the CDs could be used as an antioxidant to remove superoxide anions ($O2^-$) and hydroxyl radicals (–OH). The linear range of CDs concentrations for superoxide anion and hydroxyl radicals were 0 - 300 mg/mL and 0 - 14 mg/mL, respectively. In addition, the CDs could be a fluorescnet reagent in bioimaging of beer yeast, mould and onion skins. The favorable pH, optical properties, antioxidant ability, and bioimaging ability ensure the CDs can be exploited in food analysis and other fields.

Keywords

additive; water; detection; analysis; antioxidant

1 Introduction

Carbon dots (CDs), as a very useful nano fluorescent material, have been applied in many studies. One application of CDs is used for metal ions detection, such as Fe^{3+} [1-2], Hg^{2+} [3], Al^{3+} [4], Cu^{2+} [5], Cr^{6+} [6], Pb^{2+} [7], Co^{2+} [8], etc. Anion analysis can also be achieved by CDs, such as I^- [9], F^- [4], CN^- [10], ClO^- [11], etc. One of important applications is analysis of biological samples and drugs. For example, the CDs have been used for detecting of some drugs, such as Metronidazole [12], Hemoglobin [13], Glutathione [14], etc. Meanwhile these drugs could be delivered by CDs [15-17]. Moreover, CDs could be made to multifarious fluorescence ink, used for anti-counterfeiting [18] and cell imaging [19-20]. From the above analysis, we can see that the CDs have so many properties, we should pay

more attention to the practical application value of CDs.

pH directly affects the progress speed and balance of the chemical response. Be one of the important indicators for maintaining biological cells, it is of great significance to identify the pH of the solution [21]. Conventional approaches for pH detection are use of pH meter and pH test paper [22]. Although the instrumental approaches are more accurate, they are not suitable for the detection of pH in the organism and it is more difficult to monitor the pH change in real time. Fluorescence detection is a new method and do not cause damage to the organism, meanwhile the fluorescence materials are easier to enter organisms, therefore, more and more attentions have been paid to this method. As a new fluorescent material, CDs have been used to detect of pH in aqueous solutions [23-24].

Food additives, such as coloring reagents, flavor reagents, are widely used in the field of food processing. These additives are mostly synthetic and have a lot of potential harms to human health [25]. The existing detection methods mainly use various analytical instruments. For the detection of food additives, some analytical instruments are expensive and need to be sampled first and follow by cumbersome preparation methods [26-27]. It is of great significance to develop a simple, safe and fast method for the detection of food additives to ensure food safety.

Among food additives, antioxidants have been widely applied in the foods production. Some studies have reported that superoxide anions (O_2^-) and hydroxyl radicals (–OH) play an important role in the oxidation and modification of foods components [28-29]. Excessive free radicals might directly lead to food corruption or damage to normal cells in the human body. Therefore, more and more people began to study how to remove the radicals, and

some progresses have been made [30].

In this article, one kind of green-emission CDs was synthesized with the material m-phenylenediamine, Hydroxymethyl aminomethane (tris), phosphoric acid and pure water. The CDs exhibited green-emission fluorescence and were found to be sensitive to pH (the linear range of pH was from 3 to 10), the CDs were successfully used to evaluate the pH of aqueous solution. Besides, the CDs could detect of lemon yellow which is often used for the coloring of foods, and could be used as an antioxidant to remove superoxide anions and hydroxyl radicals. By this study, we have synthesized the multifunctional CDs, and make the CDs play a bigger role in detection and analysis.

2 Materials and Methods

We declare that the experimental procedures were in accordance with the ethical standards of the responsible committee on human experimentation.

2.1. Materials

$Zn(NO_3)_2$, $Hg(Ac)_2$, $AgNO_3$, $NiCl_2$, $CoCl_2$, $Pb(NO_3)_2$, $Fe_2(SO_4)_3$, $MgCl_2$, $AlCl_3$, LiCl, $BaCl_2$, $MnCl_2$, $CrCl_3$, NaCl, KNO_3, $CaCl_2$, $CuCl_2$ were obtained from Xinbao fine chemical company (Tianjin, China). M-phenylenediamine was produced by Jiaxing Wilbur Composites Co., LTd. (Jiaxing, China). Tris was produced by Dongguan Liaobu Runda Chemical Reagent Co., LTd. (Dongguan, China). Phosphoric acid was purchased from Beijing Beihua Fine Chemicals CO., LTD. All chemicals were analysis pure.

2.2. Characterization

Hitachi H-7700 (Hitachi, Japan) was used to analyse the transmission electron microscopy (TEM). UV-2000 UV-vis spectrophotometer (Unico, China) was used to detect UV-vis absorption spectra. F-4600 (Hitachi, Japan) was used to detect the fluorescence intensities. Bruker AXS (German) was used to analyse the X-ray diffraction (XRD) pattern. ReactIR 15 spectrometer (Mettle, Switzerland) was used to detect the Fourier transform infrared spectroscopy (FTIR) spectrum. Fluorescence microscopy (Nikon Fluophot) was used in bioimaging. The pH of the solution was adjusted by 231-01 pH meter (Shanghai Yidian, China). Quantum yields were detected by the reference method [31], the excitation wavelength was set as 440 nm, and the fluorescence results were recorded at 514 nm.

2.3. Synthesis of the CDs

The synthetic method was described as below: 25 mL of water solution containing 0.2 g m-phenylenediamine, 0.2 g tris, and 1 mL phosphoric acid were dissolved into 25 mL pure water, transfered to 50 mL Teflon-lined autoclave and heated for 8 h at 180 ℃. When the reaction temperature returned to room temperature, all the obtained materials were removed large impurities by centrifugation, and the supernatant was dialyzed by using a dialysis membrane with molecular weight cut-off of 1000 Da for 24 h. Finally, the CDs were removed excess organic solvents by vacuum distillation at 60 ℃ and acquired solids by freeze drying [32-33].

2.4. Detection of lemon yellow

Phosphate buffer solution (PBS) was used for all the detection work. A series of different concentrations of lemon yellow were added into the CDs solution, the

concentration of CDs was 0.03 mg·mL^{-1} and its pH was adjusted to neutral. The reaction solution was excited at 440 nm, and the the fluorescence intensities at 514 nm were recorded to conduct various analysises.

The recovery experiment of lemon yellow was pursued. Different concentrations of lemon yellow were spiked in tap water and lake water. The lake water was collected from the nearby lake and tap water samples were obtained from the tap pipe in our laboratory. The larger particles were removed by centrifugation, the smaller particles were removed by using a microporous membrane (internal diameter was 0.22 μm).

2.5. Antioxidant capacity analysis

Antioxidant capacity analysis included of scavenging of superoxide anion and hydroxyl radical. In the scavenging of superoxide anion experiment, phenyltriphenols self oxidation method was used. The absorbance value was determined at 325 nm. The self oxidation rate was calculated by using the Tris-HCl buffer solution (pH = 8.2) as blank. Scavenging rate of superoxide anion was calculated according to the formula (1).

$$\text{Scavenging rate}\,(\%) = (A_{\text{Blank}} - A_{CDs}) / A_{\text{Blank}} \times 100 \qquad (1)$$

A_{Blank}: absorbance of blank sample

A_{CDs}: absorbance of CDs solution

In the scavenging of hydroxyl radical experiment, the first test tube was added by 0.2 mol/L PBS (pH = 7.4), and 0.2 mL 520 mg/L safranine solution was added. The other 8 test tubes were added by 1.0 mL 0.2 mol/L PBS (pH = 7.4), 0.2 mL 520 mg/L safranine solution,

and 1.0 mL EDTANa^{2+}Fe^{2+}. Then the distilled water (7, 6, 5, 4, 3, 3, 3, 0 mL) was added, respectively. Finally 0.8 mL 6% H_2O_2 solution was added, with heated 30 min in water bath pot, the absorbance value at 520 nm was measured. Scavenging rate of hydroxyl radical was calculated according to the formula (2).

$$\text{Scavenging rate}(\%) = (A_{CDs} - A_{Blank})/(A_{Contrast} - A_{Blank}) \times 100 \quad (2)$$

A_{CDs}: absorbance of CDs

A_{Blank}: absorbance of blank

$A_{Contrast}$: absorbance of contrast

3. Results

3.1 Characterization

The synthesis principle of CDs was deduced that the amino groups of m-phenylenediamine dehydrated with the hydroxyl group of Tris, the role of phosphoric acid was to dop phosphorus in the reactants, some literatures have reported that doping phosphorus would give CDs better properties [34-36]. The morphology of the CDs was analysed by TEM. For CDs, the size was irregular and aggregated within a certain range (Figure 1a), the average diameter was measured to be 2.87 ± 0.35 nm (Figure 1b).

Surface functional groups of CDs was analysed by FTIR (Figure 1c). The peak at 1169 cm^{-1} was –C–O [37]. The absorption peaks at 1389, 1509, and 1636 cm^{-1} belonged to –C-N, –N-H, and –C=O, respectively [32]. The broad peak at 3487 cm^{-1} was ascribed to –OH [33].

The inner three-dimensional structure was analysed by X-ray diffraction (XRD). As depicted in Figure 1d, a broad peak whose central position was at 27.6°, similar to 002 facets of graphitic carbons [32, 33, 38].

Figure 1

3.2 Optical analysis

UV-vis absorption spectrum was used to analyse the bonding types of CDs (Figure 2a). There were two peaks at 360 nm and 440 nm, might attribute to π–π* and n–π* transitions, respectively [39, 40].

The fluorescence intensities of CDs were recorded at different wavelengths from 340 to 460 nm (Figure 2b). When the excitation wavelength was 440 nm, the fluorescence intensity could reach to maximum, the wavelength position here was 514 nm. The QYs were calculated to be 22.2 % using Rhodamine 6G method.

Figure 2

The photostability of CDs was compared. By experiment, it was seen that the fluorescence intensities of the CDs were stabilized within 60 min, it indicating that CDs exhibited optical stability (Figure 3a). Ionic strength directly affected the feasibility of pH regulation and other reaction operations. We compared the differences of fluorescence intensities by adding different amounts of NaCl from 0 to 400 mM. Figure 3b depicted that the detection would not be disturbed by ionic strength. The influence of temperature was investigated. The CDs exhibited good thermal stability when the temperature was changed from 30 °C to 60 °C (Figure 3c).

Figure 3

We evaluate the effects of reaction reagents on the fluorescence intensities. For example, metal ions (Figure 4a), included of 18 common metal ions, 9 kinds of anions (Figure 4b), and some interferences (Figure 4c), included of Galactose, Uric acid, VC, Valine, Thiourea, Dopamine, Maltose, Lysine, Phenylalanine, Malic acid, Threonine, Alanine, Serine, Imidazole, Tyrosine, Glutamate, Glutathione, Glucose, Glycine, Aspartic acid, Proline, Xylose. The fluorescence of the CDs was recorded in PBS at pH 3.0. The results showed that no matter metal ions, anions, or interferences, had little effect on CDs.

Figure 4

3.3 Sensing for pH in the actual water samples

The effect of pH on the CDs was depicted in Figure 5. It was seen that when pH was changed from 3 to 10, the fluorescence intensities decrease linearly with increasing pH, a linear relationship between the fluorescence intensities and pH was fitted: Fluorescence intensity = 1000.760 – 59.5849 pH (R^2 = 0.993). According to the sensitivity of CDs to pH, we used CDs to detect pH in water samples (Table. 1). We chose tap water, lake water and mineral water for testing, using the pH meter for reference. By experiments, we measured the pH values of three kinds of water samples were 8.06, 7.56, and 7.73, respectively. By comparing with the pH meter, the relative standard deviation (RSD) of three water samples were less than 5 %, so we initially believe that the synthesized CDs can be used to evaluate the pH in water.

Figure 5

Table 1

3.4 Lemon yellow sensor based on the CDs

As shown in Figure 6a, the yellow line was Uv-vis spectrum of lemon yellow. It was seen that there were two bands (260 nm, 430 nm). The optimum excitation wavelength and emission wavelength of the CDs were 440 nm (the red line) and 514 nm (the green line). The excitation wavelength (440 nm) was coincidence with UV-vis band (430 nm) of lemon yellow. When lemon yellow was spiked into the CDs solution, the excitation fluorescence was shielded by the UV-vis band of the lemon yellow, which caused the inner filter effect (IFE) occured. Figure 6b depicts the quenching time of lemon yellow, it is seen that quenching reaction needs a shorter time.

The effects of different concentrations (0 to 80 μM) of lemon yellow on CDs were shown in Figure 6c. It was seen that CDs were gradually quenched with the increase of lemon yellow. Within the scope of 0 to 16 μM, a linear equation was fitted to: $(F^0 – F)/F^0 = 0.0468 + 0.0224C$ ($R^2 = 0.9975$) (Figure 6d), where F^0 was the fluorescence intensity of initial CDs solution, F was the fluorescence intensities when lemon yellow was added into the CDs solution, and C was the concentration of lemon yellow, respectively. The limit of detection (LOD) was calculated to be 0.13 μM.

Figure 6

Table 2

3.5 Evaluate of the antioxidant of the CDs

In our study, we used CDs to scavenge superoxide anions and hydroxyl radicals to evaluate the antioxidant ability of CDs.

3.5.1 Scavenging of superoxide anions

As the concentration of CDs increased, the scavenging rate of superoxide anions was gradually increased, when the concentration of CDs reached 500 mg/mL, the scavenging rate of CDs on superoxide anions was close to equilibrium (Figure 7a). For the CDs, within the scope of 0 to 300 mg/mL, a linear equation was fitted to: Scavenging rate = – 0.4724 + $0.1310C_{CDs}$ (R^2 = 0.9991). The mechanism for scavenging of superoxide anions was deduced that the superoxide anion was very oxidizing, but when the CDs were added into the superoxide anions solution, the superoxide anions would passivate the surface. The functional groups play a big role in the fluorescence generation, because the surface functional groups were oxidized, so the fluorescence of CDs was quenched [41-43].

Figure 7

3.5.2 Scavenging of hydroxyl radical

The scavenging effect of CDs on hydroxyl radicals was also researched (Figure 8). Within the scope of 0 to 14 mg/mL, a linear equation was fitted to：Scavenging rate = $4.6714 + 4.4325C_{CDs}$, (R^2 = 0.9924). The mechanism for scavenging of hydroxyl radical was deduced that green-emission CDs were synthesized using phosphoric acid as a raw material, phosphoric acid contains a lot of protons, they are easily absorbed the surface of the CDs. When these protons encountered hydroxyl radicals, these protons could react with

the hydroxyl radicals to produce water [28, 29]. Due to the depletion of protons, the surface of the the CDs was modified, so the fluorescences were quenched.

Figure 8

3.6 Fluorescence bioimaging of the CDs

In order to verify the toxicity of CDs and explore the application of CDs in bioimaging. Beer yeast, mildew and onion skins were selected as the medium for imaging. Fluorescence microscopy was used to visualize the CDs label. Beer yeast has very small cell structure. It was seen that yeast cells are lit up by fluorescence (Figure 9). The mycelium of the mildew has a fluffy structure. It was seen that the CDs have entered the gap between the mycelia (Figure 10). The onion epidermal cells had a wide range of results, and the fluorescent substances were mainly concentrated in the gap between the cells (Figure 11). The imaging results indicated that the CDs are less toxic and does not destroy the cell, could be used for bioimaging.

Figure 9

Figure 10

Figure 11

Conclusionn

In this paper we used the facile method to synthesize CDs, the CDs could sense for the pH of tap water, lake water and mineral water. Meanwhile the CDs could detect of lemon yellow via the mechanism IFE, meanwhile the synthesized CDs could effectively remove

superoxide anions and hydroxyl radicals, which shows that the CDs can be used for potential antioxidant applications. In additon, the CDs could be used in bioimaging of beer yeast, mildew and onion skins. Because of the CDs' many excellent characteristics, we believe that the CDs will have broad application prospects. For its practical application, we will further explore in the further study.

Acknowledgments

This work was financially supported by National Natural Science Foundation of China (project number: U1860112), Natural Science Foundation of Liaoning Province (project number: 20170520093, 20170540466), Foundation of Liaoning Province Education Administration (project number: 2017FWDF05).

Conflict of interest

Authors declare no conflicts of interest.

References

1. Li, G. M.; Lv, N.; Bi, W. Z.; Zhang, J. L.; Ni, J. Z. *New Journal of Chemistry*, **2013,** 00:1-3.

2. Ge, L.; Yu, H. L.; Ren, H. T.; Shi, B.; Guo, Q.; Gao, W. S.; Li, Z. Q.; Li, J. G. *Journal of Materials Science*, **2017,** 52, 9979-9989.

3. Gu, D.; Shang, S. M.; Yu, Q.; Shen, J. *Applied Surface Science*, **2016,** 390, 38-42.

4. Sun, X. Y.; Wu, L. L.; Shen, J. S.; Cao, X. G.; Wen, C. J.; Liu, B.; Wang, H. Q. *RSC Advances*, **2016,** 6, 97346-97351.

5. Amjadi, M.; Manzoori, J. L.; Hallaj, T.; Azizi, N. Journal of Luminescence, **2017,** 182, 246-251.

6. Bu, L. L.; Peng, J. D.; Peng, H. J.; Liu, S. P.; Xiao, H.; Liu, D.; Pan, Z. Y.; Chen, Y.; Chen, F.; He, Y. *RSC Advances*, **2016,** 6, 95469-95475.

7. Jiang, Y. L.; Wang, Y. X.; Meng, F. D.; Wang, B. X.; Cheng, Y. X.; Zhu, C. *J. New Journal of Chemistry*, **2015,** 39, 357-3360.

8. Geng, S.; Lin, S. M.; Shi, Y.; Li, N. B.; Luo, H. Q. *Microchimica Acta*, **2017,** 184, 2533-2539.

9. He, J. L.; Zhang, H. R.; Zou, J. L.; Liu, Y. L.; Zhuang, J. L.; Xiao, Y.; Lei, B. F. *Biosensors and Bioelectronics*, **2016,** 79, 531-535.

10. Zhang, J.; Dong, L.; Yu, S. H. *Science Bulletin*, **2015,** 60, 785-791.

11. Wang, D. M.; Xu, H.; Zheng, B. Z.; Li, Y.; Liu, M. P.; Du, J.; Xiao, D. *Analytical Methods*, **2015,** 7, 5311-5317.

12. Zhao, J. R.; Pan, X. H.; Sun, X. B.; Pan, W.; Yu, G. F.; Wang, J. P. Journal of *Luminescence*, **2018,** 33, 1-9.

13. Barati, A.; Shamsipur, M.; Abdollahi, H. *Biosensors and Bioelectronics*, **2015,** 71, 470-475.

14. Gu, J. J.; Hu, D. H.; Wang, W. N.; Zhang, Q. H.; Meng, Z.; Jian, X. D.; Xi, K. *Biosensors and Bioelectronics*, **2015,** 68, 27-33.

15. Li, S. H.; Amat, D.; Peng, Z. L.; Vanni, S.; Raskin, S.; Angulo, G. D.; Othman, A. M.; Graham, R. M.; Leblanc, R. M. *Nanoscale*, **2016,** 8, 16662-16669.

16. Ding, H.; Du, F. Y.; Liu, P. C.; Chen, Z. J.; Shen, J. C. *ACS Applied Materials & Interfaces*, **2015,** 7, 6889-6897.

17. Feng, T.; Ai, X. Z.; An, G. H.; Yang, P. P.; Zhao, Y. L. *ACS Nano*, **2016,** 10, 4410-4420.

18. Lou, Q.; Qu, S. N.; Jing, P. T.; Ji, W. Y.; Li, D.; Cao, J. S.; Zhang, H.; Liu, L.; Zhao, J. L.; Shen, D. Z. *Advanced Materials*, **2015,** 27, 1389-1394.

19. D’souza, S. L.; Deshmukh, B.; Bhamore, J. R.; Rawat, K. A.; Lenka, N.; Kailasa, S. K. *RSC Advances*, **2016,** 6(15), 12169-12179.

20. Sun, R.; Yin, L.; Zhang, S. H.; He, L.; Cheng, X. J.; Wang, A. N.; Xia, H. W.; Shi, H. B. *Chemistry-A European Journal*, **2017,** 23, 1-5.

21. Chowdhuri, A. R.; Singh, T.; Ghosh, S. K.; Sahu, S. K. *ACS Applied Materials & Interfaces*, **2016,** 8(26), 16573-16583.

22. Barati, A.; Shamsipur, M.; Abdollahi, H. *Analytica Chimica Acta*, **2016,** 931, 25-33.

23. Gui, R. J.; Ana, X. Q.; Huang, W. X. *Analytica Chimica Acta*, **2013,** 767, 134-140.

24. Wang, W. J.; Xia, J. M.; Feng, J.; He, M. Q.; Chen, M. L.; Wang, J. H. *Journal of Materials Chemistry B*, **2016,** 4, 7130-7137.

25. Kim, H. J.; Lee, M. J.; Park, H. J.; Kim, H. J.; Cho, S. K.; Jeong, M. H. *Food Science and Biotechnology*, **2018,** 27(3), 877-882.

26. Ma, K.; Li, X. J.; Wang, H. F.; Zhao, M. *Food Analytical Methods*, **2015,** 8, 203-212.

27. Zhao, H. P.; Sun, W. L.; Wang, Z.; Zhang, T.; Fan, Y. Y.; Gu, H. J.; Li, G. Y. *Current Microbiology*, **2017,** 74, 1169-1177.

28. Costas-Mora, I.; Romero, V.; Lavilla, I.; Bendicho, C. *Talanta*, **2015,** 144, 1308-1315.

29. Sachdev, A.; Gopinath, P. *The Analyst*, **2015,** 140(12), 4260-4269.

30. Shen, J.; Shang, S. M.; Chen, X. Y.; Wang, D.; Cai, Y. *Sensors and Actuators B*, **2017,** 248, 92-100.

31. Grabolle, M.; Spieles, M.; Lesnyak, V.; Gaponik, N.; Eychmuller, A.; Resch-Genger U. *Analytical Chemistry*, **2009,** 81, 6285-6294.

32. Li, C.; Liu, W. J.; Ren, Y. J.; Sun, X. B.; Pan, W.; Wang, J. P. *Sensors and Actuators B*, **2017,** 240, 941-948.

33. Li, C.; Liu, W. J.; Sun, X. B.; Pan, W.; Yu, G. F.; Wang, J. P. *Sensors and Actuators B*, **2018,** 263, 1-9.

34. Sarkar, S.; Das, K.; Ghosh, M.; Das, P. K. *RSC Advances*, **2015,** 5(81), 65913-65921.

35. Shi, B. F.; Su, Y. B.; Zhang, L. L.; Huang, M. J.; Liu, R. J.; Zhao, S. L. *ACS Applied Materials & Interfaces*, **2016,** 8, 10717-10725.

36. Shi, D.; Yan, F.; Zheng, T.; Wang, Y.; Zhou, X.; Chen, L. *RSC Advances*, **2015,** 5(119), 98492-98499.

37. Bojdys, M. J.; Muller, J. O.; Antonietti, M.; Thomas, A. *Chemistry-A European Journal*, **2008,** 14, 8177-8182.

38. Vikneswaran, R.; Ramesh, S.; Yahya, R. *Materials Letters*, **2014,** 36, 179-182.

39. Lan, M. H.; Di, Y. F.; Zhu, X. Y.; Ng, T. W.; Xia, J.; Liu, W. M.; Meng, X. M.; Wang, P. F.; Lee, C. S.; Zhang, W. J. *Chemical Communications*, **2015,** 51, 15574-15577.

40. Liu, M.; Xu, Y.; Niu, F.; Gooding, J. J.; Liu, J. *Analyst*, **2016,** 141, 2657-2664.

41. Wang, D.; Liu, J. Y.; Chen, J. F.; Dai, L. M. *Advanced Materials Interfaces*, **2016,** 3, 1-6.

42. Wang, Z. G.; Long, P.; Feng, Y. Y.; Qin, C. Q.; Feng, W. *RSC Advances*, **2017,** 7, 2810-2816.

43. Xu, X. Y.; Bao, Z. J.; Tang, W. S.; Wu, H. Y.; Pan, J.; Hu, J. G.; Zeng, H. B. *Carbon*, **2017,** 121, 201-208.

Table 1: Analytical results for the detection of pH in real water samples.

Sample	pH value by pH meter	pH value by CDs[a]	RSD (%)[b]
Tap water	8.06	7.82 ± 0.19	3.02
Lake water	7.56	7.23 ± 0.24	4.46
Mineral water	7.73	7.44 ± 0.13	3.82

[a] Results were expressed as the mean of three determinations ± standard deviation (SD).

[b] Relative standard deviation (RSD) was defined as (SD/mean) × 100%.

Table 2: Analytical results for the detection of lemon yellow in real water samples.

Sample	Spiked concentration (μM)	Total found (μM)	Recovery (%) N=3	RSD (%) N=3
Tap water	3.8	3.671	96.61	0.66
	8.0	8.007	100.09	0.89
	10	9.990	99.90	0.61
Lake water	3.8	3.769	99.18	0.61
	8.0	8.069	100.86	0.10
	10	10.626	106.26	4.09

Figure Captions:

Figure 1(a) TEM image (b) particle size distribution (c) XRD pattern and (d) FTIR spectrum of the CDs.

Figure 2(a) The UV-Vis absorption spectrum, excitation spectrum monitored at 440 nm and emission spectrum excited at 514 nm of the as-prepared CDs. Inset: the photograph of the CDs in aqueous solution under illumination of sunlight (left) and UV light (365 nm, right). (b) Fluorescence spectra of the as-prepared CDs (recorded from 340 to 460 nm with an increment of 20 nm).

Figure 3(a) The photostability of the CDs fluorescence intensity under the constant irradiation at 440 nm. (b) The effect of ionic strength (NaCl solution at concentration of 0, 25, 50, 100, 200, 400 mM, respectively). (c) The effect of temperature on the fluorescence intensity of the CDs.

Figure 4 The selectivity of the CDs based sensor in the presence of interferences (a) metal ions (b) anion (c) other interferences.

Figure 5 The effect of the pH on the fluorescence intensity of the CDs.

Figure 6(a) The fluorescence spectra of lemon yellow excitation spectra and emission spectra of CDs (excitation wavelengths was 440 nm). (b) The quenching time of lemon yellow. (c) Fluorescence spectra of the CDs in PBS buffer solution (0.1 $mol \cdot L^{-1}$, pH 3.0) upon addition of various concentrations of lemon yellow (from top to bottom: 0 - 80 μM; the excitation wavelength was

440 nm and the emission wavelength was 514 nm). (d) The linear relationships between $(F^0–F)/F^0$ and lemon concentration (0 - 16 μM).

Figure 7 scavenging rate of superoxide anions (O_2^-) under different concentrations of CDs (the red line was all the experimental datas, the black line was the datas in the linear scope).

Figure 8 scavenging rate of hydroxyl radical (–OH) under different concentrations of CDs.

Figure 9 Fluorescence microscopic images of beer yeast soaked with CDs for 2 hours. (a) Bright fifield image. Fluorescence images taken on exciter fifilters: (b) excitation 330–385 nm, emission 420 nm (blue); (c) excitation 450–480 nm, emission 515 nm (green); (d) excitation 510–550 nm, emission 590 nm (red), respectively. Scale bar indicates 40 microns. Magnifification 40×.

Figure 10 Fluorescence microscopic images of mildew soaked with CDs for 2 hours. (a) Bright fifield image. Fluorescence images taken on exciter fifilters: (b) excitation 330–385 nm, emission 420 nm (blue); (c) excitation 450–480 nm, emission 515 nm (green); (d) excitation 510–550 nm, emission 590 nm (red), respectively. Scale bar indicates 40 microns. Magnifification 40×.

Figure 11 Fluorescence microscopic images of onion skin soaked with CDs for 2 hours. (a) Bright fifield image. Fluorescence images taken on exciter fifilters: (b) excitation 330–385 nm, emission 420 nm (blue); (c) excitation 450–480 nm,

emission 515 nm (green); (d) excitation 510–550 nm, emission 590 nm (red), respectively. Scale bar indicates 40 microns. Magnifification 40×.

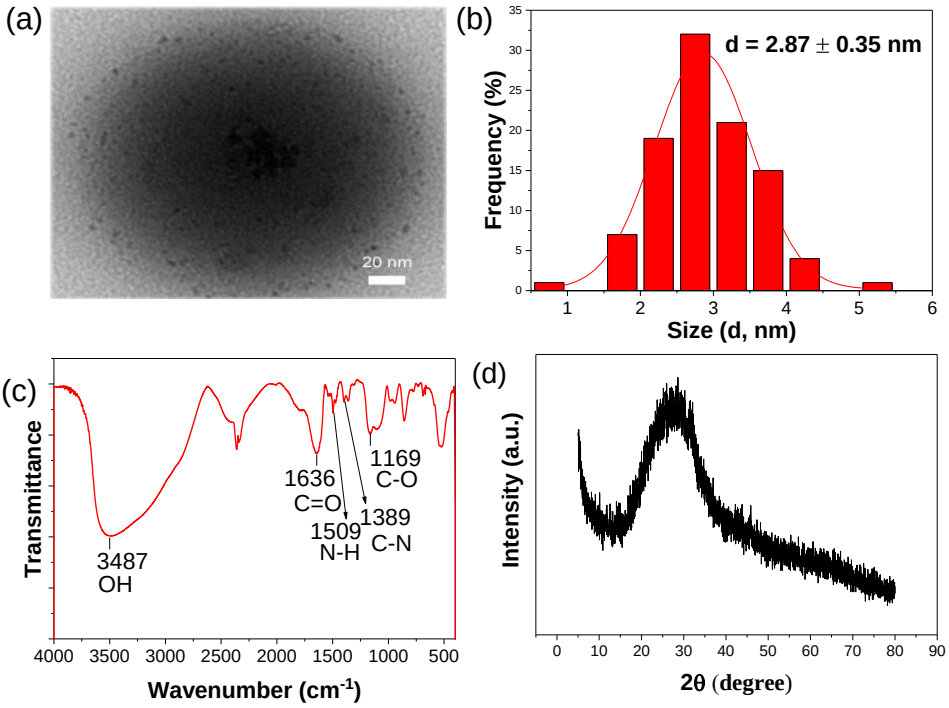

Figure 1(a) TEM image (b) particle size distribution (c) XRD pattern and (d) FTIR spectrum of the CDs.

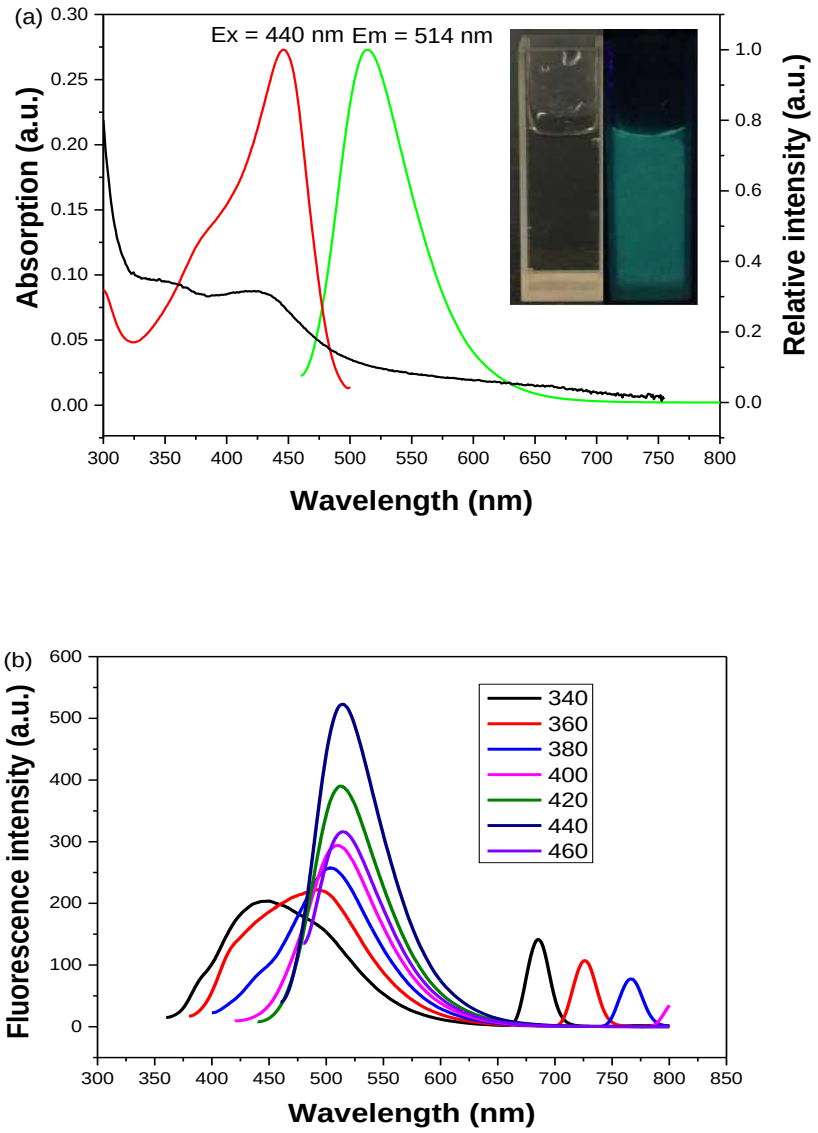

Figure 2(a) The UV-Vis absorption spectrum, excitation spectrum monitored at 440 nm and emission spectrum excited at 514 nm of the as-prepared CDs. Inset: the photograph of the CDs in aqueous solution under illumination of sunlight (left) and UV light (365 nm, right). (b) Fluorescence spectra of the as-prepared CDs (recorded from 340 to 460 nm with an increment of 20 nm).

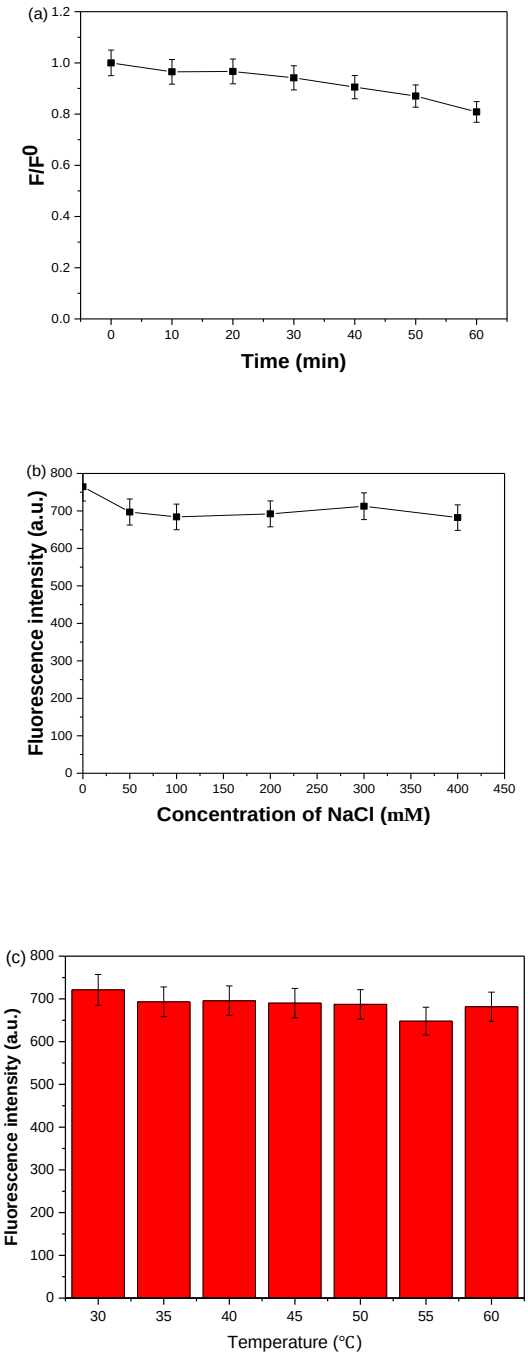

Figure 3(a) The photostability of the CDs fluorescence intensity under the constant irradiation at 440 nm. (b) The effect of ionic strength (NaCl solution at concentration of 0, 25, 50, 100, 200, 400 mM, respectively). (c) The effect of temperature (℃) on the fluorescence intensity of the CDs.

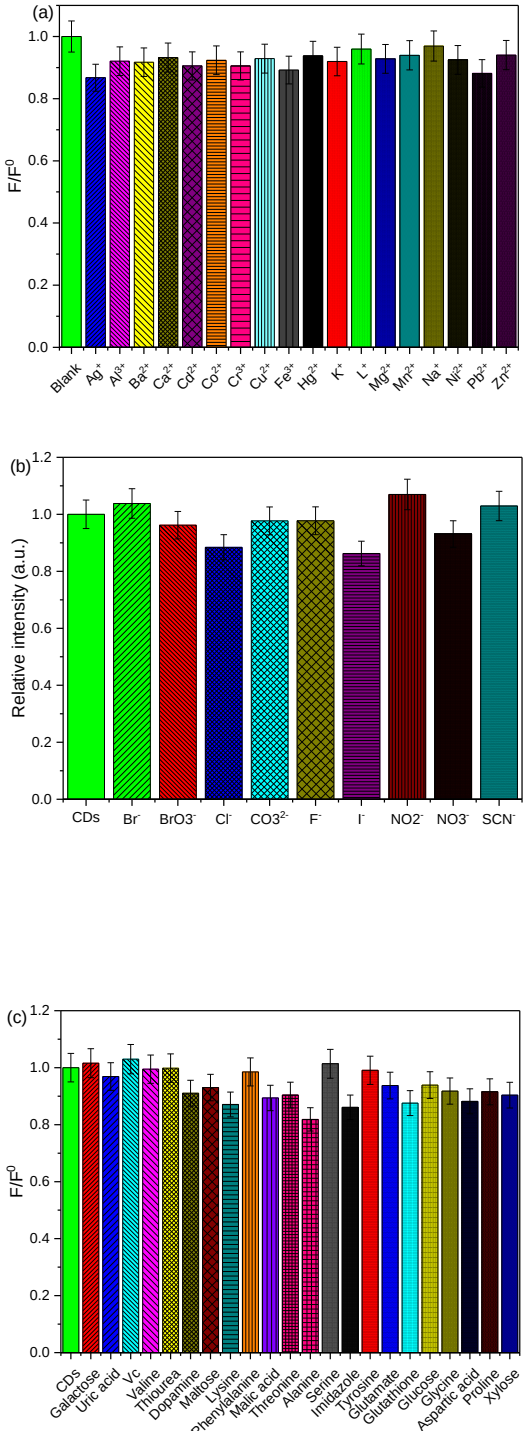

Figure 4 The selectivity of the CDs based sensor in the presence of interferences (a) metal ions (b) anion (c) other interferences.

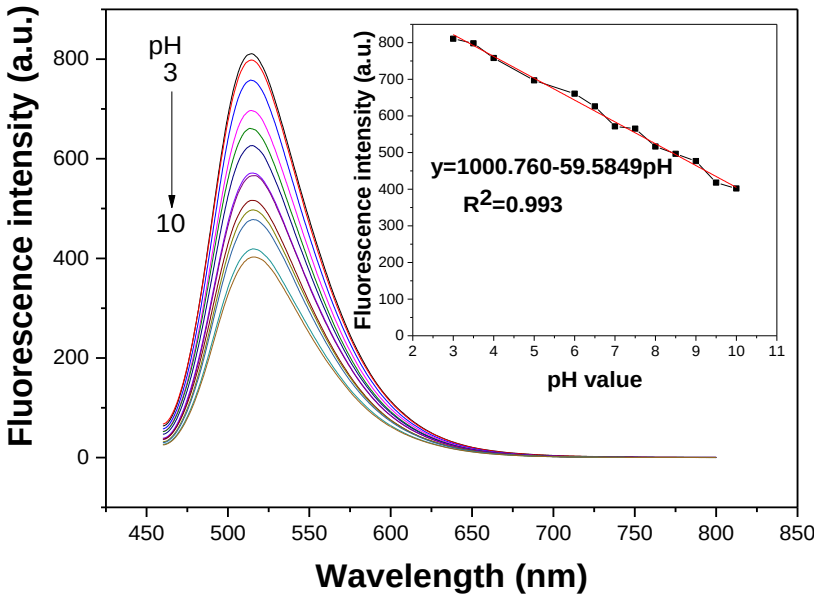

Figure 5 The effect of the pH on the fluorescence intensity of the CDs.

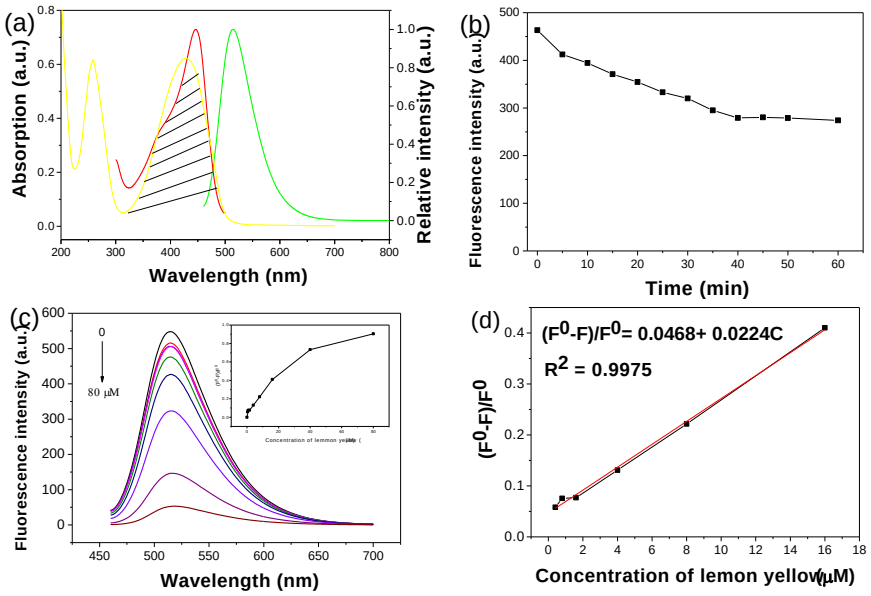

Figure 6(a) The fluorescence spectra of lemon yellow excitation spectra and emission spectra of CDs (excitation wavelengths was 440 nm). (b) The quenching time of lemon yellow. (c) Fluorescence spectra of the CDs in PBS buffer solution (0.1 mol·L^{-1}, pH 3.0) upon addition of various concentrations of lemon yellow (from top to bottom: 0 - 80 μM; the excitation wavelength was 440 nm and the emission wavelength was 514 nm). (d) The linear relationships between $(F^0–F)/F^0$ and lemon concentration (0 - 16 μM).

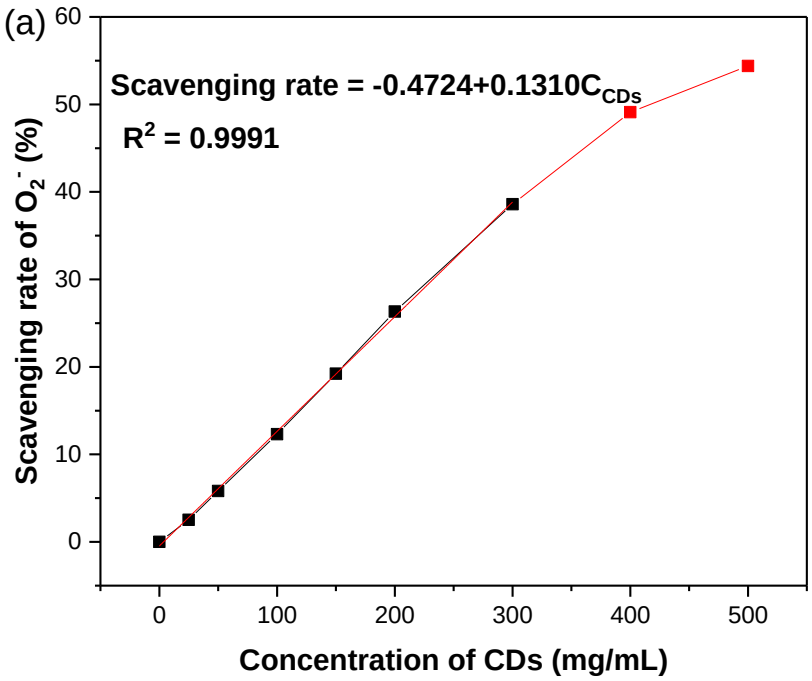

Figure 7 scavenging rate of superoxide anions (O_2^-) under different concentrations of CDs (the red line was all the experimental datas, the black line was the datas in the linear scope).

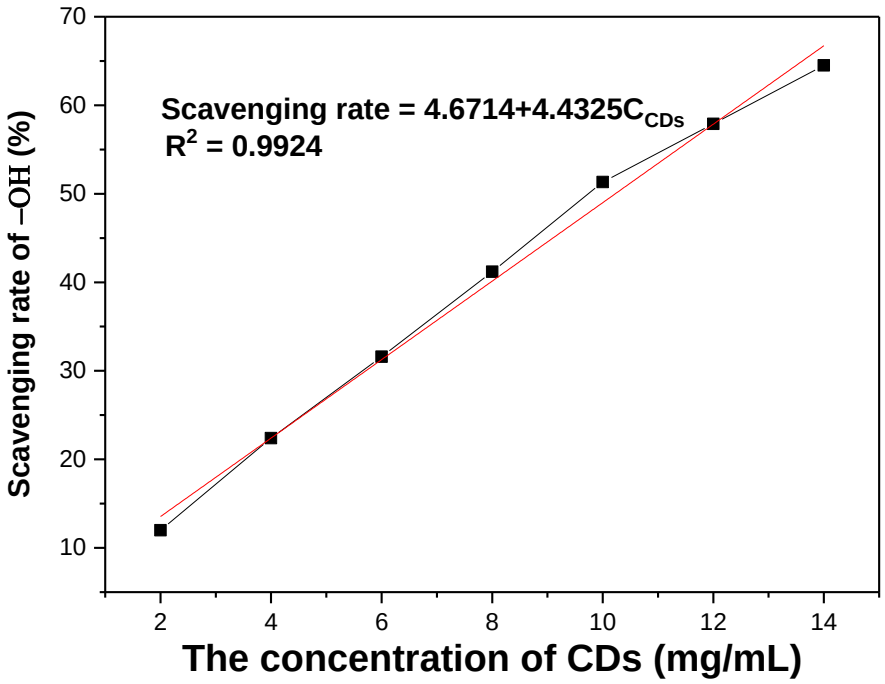

Figure 8 scavenging rate of hydroxyl radical (–OH) under different concentrations of CDs.

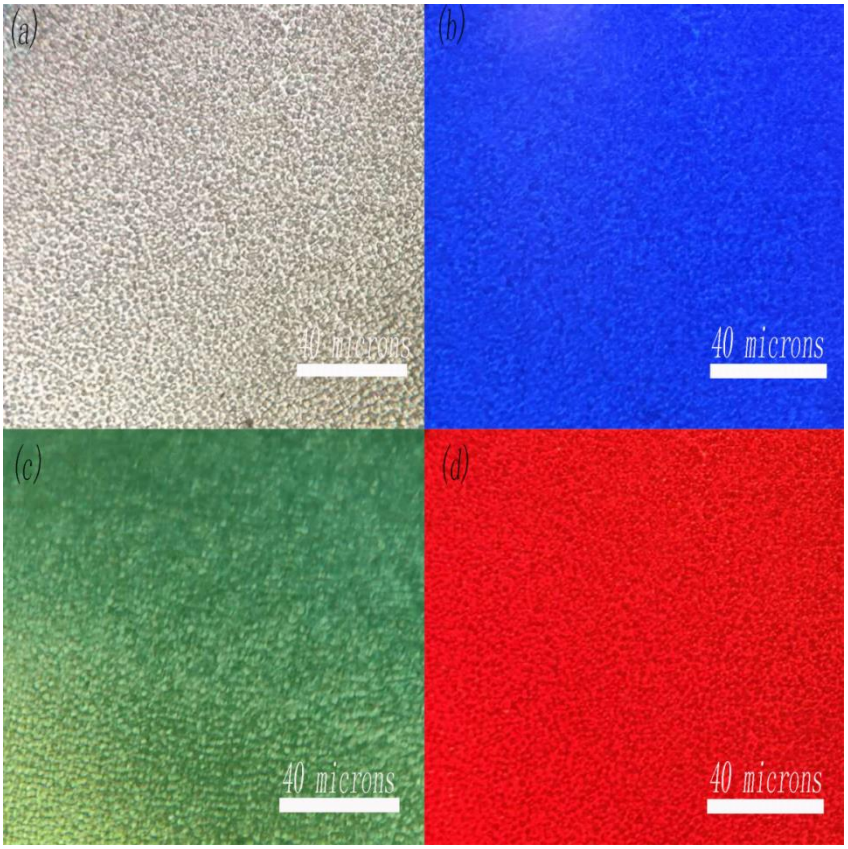

Figure 9 Fluorescence microscopic images of beer yeast soaked with CDs for 2 hours. (a) Bright fifield image. Fluorescence images taken on exciter fifilters: (b) excitation 330–385 nm, emission 420 nm (blue); (c) excitation 450–480 nm, emission 515 nm (green); (d) excitation 510–550 nm, emission 590 nm (red), respectively. Scale bar indicates 40 microns. Magnifification 40×.

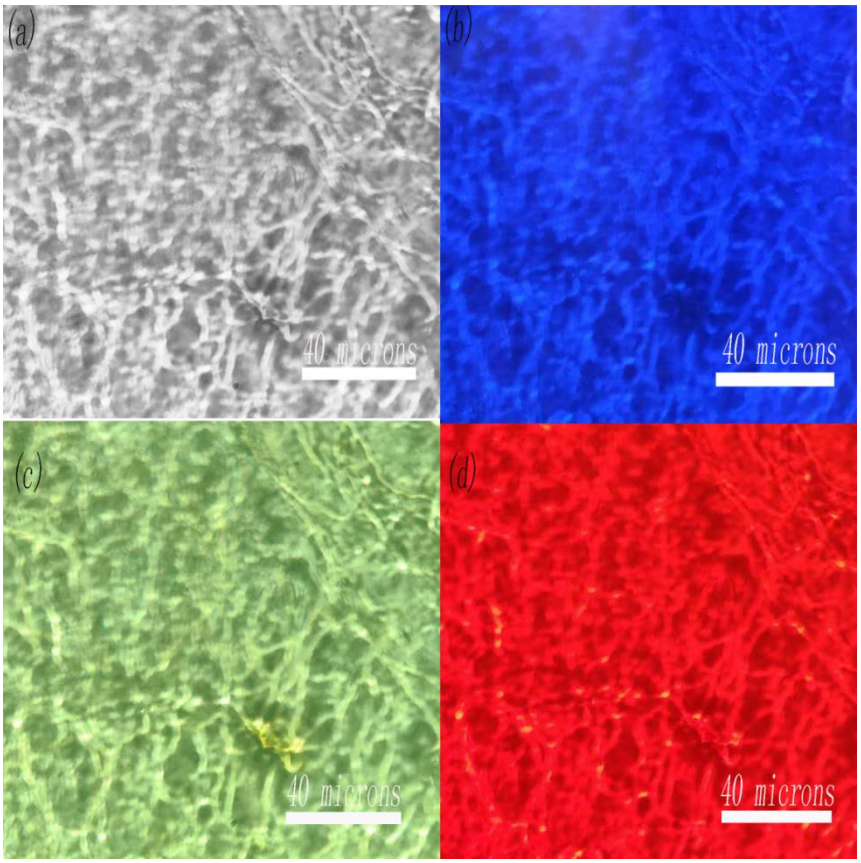

Figure 10 Fluorescence microscopic images of mildew soaked with CDs for 2 hours. (a) Bright fifield image. Fluorescence images taken on exciter fifilters: (b) excitation 330–385 nm, emission 420 nm (blue); (c) excitation 450–480 nm, emission 515 nm (green); (d) excitation 510–550 nm, emission 590 nm (red), respectively. Scale bar indicates 40 microns. Magnifification 40×.

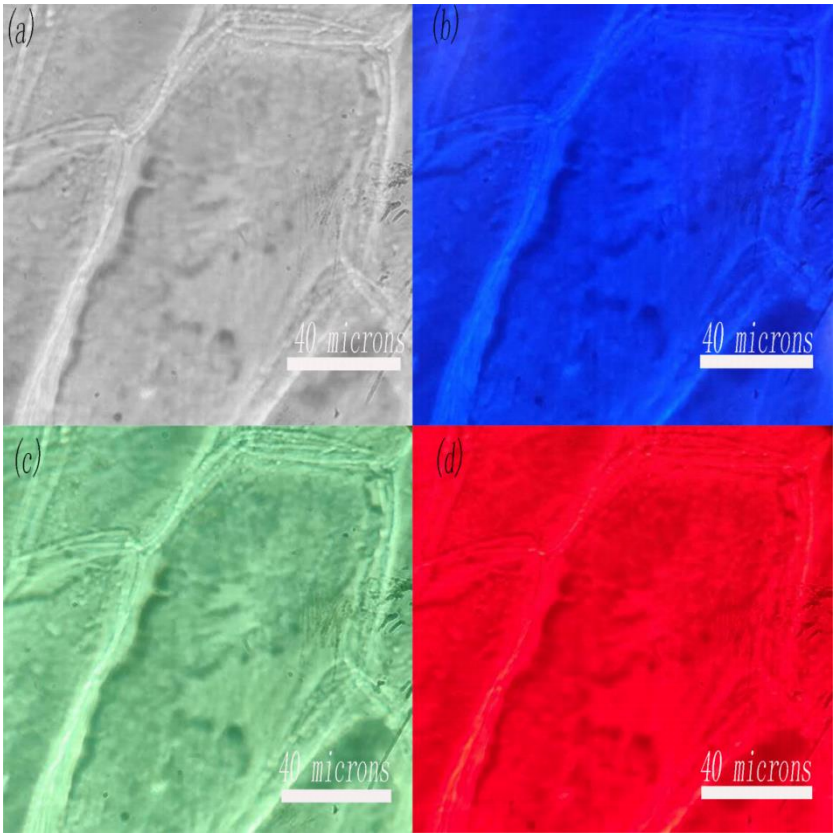

Figure 11 Fluorescence microscopic images of onion skin soaked with CDs for 2 hours. (a) Bright fifield image. Fluorescence images taken on exciter fifilters: (b) excitation 330–385 nm, emission 420 nm (blue); (c) excitation 450–480 nm, emission 515 nm (green); (d) excitation 510–550 nm, emission 590 nm (red), respectively. Scale bar indicates 40 microns. Magnifification 40×.